Nonclassical properties of electronic states of aperiodic chains in a homogeneous electric field

B. J. Spisak[1,2,*] and M. Wołoszyn[2,†]

[1]*School of Physics and Astronomy, University of Leeds, Leeds LS2 9JT, United Kingdom*

[2]*Faculty of Physics and Applied Computer Science, AGH University of Science and Technology,*
Aleja Mickiewicza 30, 30-059 Kraków, Poland

The electronic energy levels of one-dimensional aperiodic systems driven by a homogeneous electric field are studied by means of a phase-space description based on the Wigner distribution function. The formulation provides physical insight into the quantum nature of the electronic states for the aperiodic systems generated by the Fibonacci and Thue-Morse sequences. The nonclassical parameter for electronic states is studied as a function of the magnitude of homogeneous electric field to achieve the main result of this work, which is to prove that the nonclassical properties of the electronic states in the aperiodic systems determine the transition probability between electronic states in the region of anticrossings. The localization properties of electronic states and the uncertainty product of momentum and position variables are also calculated as functions of the electric field.

I. INTRODUCTION

Analysis of the electronic states of artificial structures (e.g., superlattices, quantum wires, rings, or dots) plays a central role in modern condensed-matter physics because they determine many useful properties indispensable in industrial applications of atomic-scale or nanoscale devices. The experimental realization of that kind of structures allows us to investigate the influence of quantum effects on mechanical, optical, or transport properties. The atomic cluster structures such as quantum corrals or chains can be fabricated using the low-temperature scanning tunneling microscope (STM) manipulation of individual atoms on the conducting substrate[1,2] or mechanically controllable break junction (MCBJ).[3–5] The latter method allows us to fabricate only very short monatomic or mixed atomic chains that consist of four or five metal atoms;[6,7] on the contrary, the tip of STM can be used to build longer and much more complex structures with different shapes. Additionally, long atomic chains can be reconstructed on a flat surface by self-assembly. Experimental results for self-assembled gold atomic chains on silicon surfaces confirmed the existence of long and stable chains.[8,9] In this case the chains are extended over hundreds of nanometers and can break due to atomic defects or because of the intentional removal of single atom or group of atoms from the perfect chain. It means that experimental techniques open up the possibility to fabricate metal nanostructures created by the intentional atomic rearrangement. On the other hand, the external fields interacting with electronic states of the systems can modify their electronic spectrum and properties of the system are observed. Especially the interaction with the electronic states in the system with broken translational symmetry (disordered or aperiodic systems) seems to be interesting because the quantum interference effects determine the electronic properties of the systems at low temperatures, e.g., Refs. [10–12]. One of the simplest but nontrivial examples of the interactions is the effect of the homogeneous electric field on electronic states in crystals where the Wannier-Stark quantization was predicted[13–16] and confirmed experimentally in artificial semiconductor and optical superlattices.[17–19] Discussion of the effect in one-dimensional periodic systems has been carried out for many years[20–28] and is still the subject of current experimental as well as theoretical research.[29–32]

In this paper, we apply the phase-space approach based on the nonclassical distribution functions[33–36] to the problem of electronic states in isolated and finite one-dimensional aperiodic systems generated by the Fibonacci and Thue-Morse sequences[37–39] in the presence of an external homogeneous electric field. This approach is widely used in the study of quantum transport phenomena[40–44] but less exploited in the description of electronic states of nanosystems.[45] The phase-space method allows one to carefully investigate the increasing role of the quantum effects resulting from interplay between the electric field and aperiodic ordering in the one-dimensional systems and leading to the greater importance of the nonclassical properties of electronic states. We compute the Wigner distribution functions for some electronic states in the aperiodic systems and analyze their localization properties in the phase space as a function of electric field. The analysis is based on the inverse participation ratio (IPR) in the phase space.[46,47] This approach allows us to show that the electric field increases the nonclassical properties of electronic states close to the transition between them.

The presented analysis can be simply extended to the description of cold atoms in the optical lattice[48–50] or layered systems such as aperiodic superlattices consisting of two different materials that are arranged according to appropriate aperiodic sequence, e.g., Refs. [51–53], and references therein.

The rest of the paper is organized as follows. In Sec. II, we present the theoretical model of pseudoatomic chain. In Sec. III we apply the formalism of nonclassical distribution functions to the quantitative analysis of electronic states in the aperiodic systems in the external electric field. In concluding remarks we summarize presented results.

II. THEORETICAL MODEL AND METHODS

We consider the aperiodic chain of metallic potential wells modeling atoms which can be described by the one-particle Hamiltonian in the form

$$\mathcal{H}_0 = \frac{p_x^2}{2m} + \sum_{i=1}^{N} v(x - X_i), \tag{1}$$

where m is the effective mass of electron and N is the number of wells. The positions of wells, X_i, are distributed according to the binary Fibonacci and Thue-Morse sequences. We generate these sequences over set $\{0,1\}$ using the following inflation rules:[38] (a) Fibonacci sequence: $0 \rightarrow 01$ and $1 \rightarrow 0$ and (b) Thue-Morse sequence: $0 \rightarrow 01$ and $1 \rightarrow 10$.

In our notation zero corresponds to an empty site in the simple crystal lattice and one corresponds to a site in the lattice occupied by the potential well $v(x - X_i)$. The potential term in Hamiltonian (1) is represented by the superposition of the potential wells $v(x - X_i)$. We assume that each well in the chain is given by the Shaw pseudopotential modified by screening, namely,

$$v(x - X_i) = -v_0 \begin{cases} \dfrac{\exp(-\mu|x - X_i|)}{|x - X_i|}, & |x - X_i| > x_c \\ \dfrac{\exp(-\mu x_c)}{x_c}, & |x - X_i| \leq x_c. \end{cases} \tag{2}$$

A quantity x_c is the cutoff parameter and it is chosen to have the value for which the pseudopotential reproduces the ionization energy of Cu; μ is the screening factor in the Thomas-Fermi approximation. We assume that each well gives only one state to the conduction band and therefore the Fermi level, E_F, is defined in the middle of the conduction band. Finally a constant electric field $\mathcal{E}$ is applied along the wire and the total Hamiltonian of the system under the electrostatic perturbation has a form

$$\mathcal{H} = \mathcal{H}_0 + e\mathcal{E}x, \tag{3}$$

where $-e$ is the electron charge.

The energy spectrum of the finite system, which is described by Hamiltonian (1) forms the energy bands. The structure of these energy bands strongly depends on the arrangement of potential wells. When a periodic system is subjected to the electric field, the eigenstates of Hamiltonian (3) form so-called homogeneous Wannier-Stark ladders.[13,54] This situation is presented in Fig. 1(a). In the aperiodic structures generated by the Fibonacci and Thue-Morse order, the eigenstates of Hamiltonian (3) form more complex energy spectra of the conduction band as it is shown in Figs. 1(b) and 1(c).

In these cases, the electronic states tend to group into subbands. The energy widths of these subbands are much smaller than the width of the conduction band for the periodic system and strongly depend on the values of electric field and number of wells in the systems. As a result, the aperiodic systems form the inhomogeneous Wannier-Stark ladders. From these results we conclude that the effect of inhomogeneous Wannier-Stark ladders originates from the interplay between aperiodic order and the electric field on the electronic states. A closer inspection of the inhomogeneous
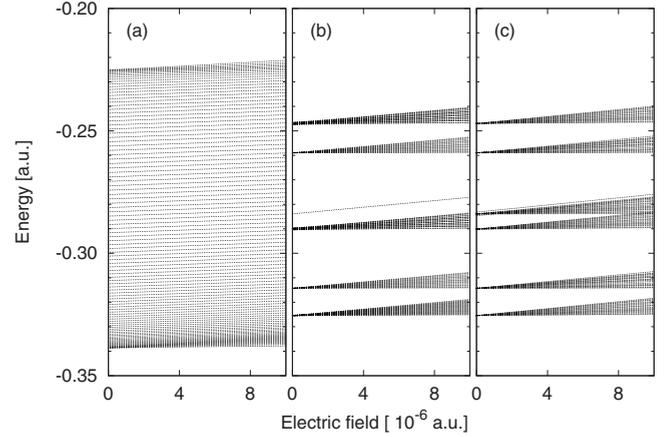

FIG. 1. Energies of states in the conduction band for $N=100$ wells as a function of the electric field for (a) periodic, (b) Fibonacci, and (c) Thue-Morse sequence.

Wannier-Stark ladders reveals the occurrence of changes in energy levels inclinations in the electric field. These changes result from the repulsion between neighboring electronic states and the anticrossings[55] are observed between them for some values of the electric field as it is shown in Fig. 2.

These nontrivial properties of the inhomogeneous Wannier-Stark ladders suggest that the correlated position and momentum behavior of electronic states play an important role in the region of anticrossings. Therefore the nature of these electronic states is analyzed by the phase-space methods. Here, we restrict ourselves to the detailed analysis of the states in the vicinity of the band bottom but we also present briefly some results for the states in the middle of the conduction band.
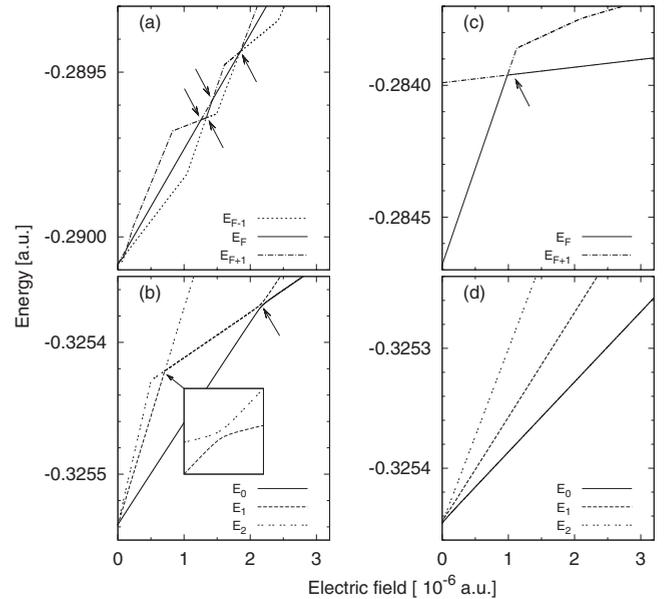

FIG. 2. Energies calculated for [(a) and (b)] the Fibonacci sequence and [(c) and (d)] Thue-Morse sequence. (a) and (c) show states at the Fermi level (E_F) and directly below and above the Fermi level (E_{F-1} and E_{F+1}, respectively). (b) and (d) show states at the bottom of the conduction band. Arrows point to the anticrossings.

Within the phase-space approach, the electronic states may be represented by the Wigner distribution function. For an electron in the pure state the Wigner distribution function has the form[33–35]

$$f_n(x,k) = \int dx' \left\langle x - \frac{1}{2}x' \middle| \psi_n \right\rangle \left\langle \psi_n \middle| x + \frac{1}{2}x' \right\rangle e^{ikx'}. \quad (4)$$

It should be noted that the Wigner distribution function is a bilinear combination of the electron wave function and therefore contains interference information. By means of the Wigner distribution function we can evaluate the expectation value of any Hermitian quantum-mechanical operator $\mathcal{A}$ in the state n using the formula[33,35]

$$\langle A \rangle_n = \int dx\, dk\, A(x,k) f_n(x,k), \quad (5)$$

where $A(x,k)$ is the Wigner representation of quantum-mechanical operator $\mathcal{A}$ given by

$$A(x,k) = \int dx' \left\langle x - \frac{1}{2}x' \middle| \mathcal{A} \middle| x + \frac{1}{2}x' \right\rangle e^{ikx'}. \quad (6)$$

Because the Wigner distribution function can take negative values in some subregions of the phase space it cannot be interpreted as the classical distribution function in the phase space. The negative part of the Wigner distribution function is responsible for quantum correlations between spatially separated pieces of the electronic state.[56] It stems from the fact that the information from the off-diagonal terms in Eq. (4) represented by $x' \neq 0$ variable is transferred to the Wigner distribution function via the momentum k. These properties characteristic for the Wigner distribution function may be utilized as an indicator of nonclassicality of electronic states.[57,58]

III. RESULTS AND DISCUSSION

In the present considerations we assume that the aperiodic systems generated by the Fibonacci and Thue-Morse sequences are limited by the infinite wells. The energy spectra were calculated for weak electric fields using the parameters of the conduction electron in copper. In our calculations we consider chains of different lengths (e.g., 30, 50, or 100 potential wells). Here we present the results for 100 wells containing all characteristic properties of the obtained results. All values are given in atomic units $\hbar = |e| = m_e = 1$.

In the first step we determine the Wigner distribution functions for some of pure states and investigate their changes due to the electric field. Figure 3 shows the Wigner distribution functions for the two lowest electronic states in the Fibonacci chain in the vicinity of the first anticrossing that is pointed to by the arrow in Fig. 2(b).

Initially, both electronic states which are represented by the Wigner distribution functions $f_0(x,k)$ and $f_1(x,k)$ occupy different regions of the phase space. Increasing the electric field shifts the states in opposite directions so that the distance between them decreases. Finally, in the region of anticrossing, the Wigner distribution functions occupy the same
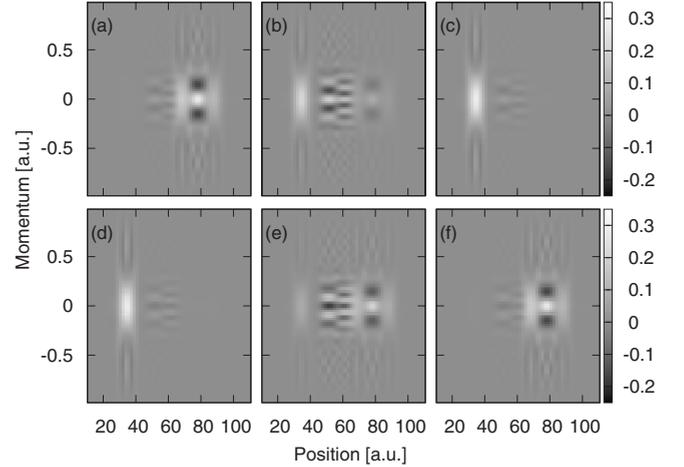

FIG. 3. The Wigner function for the system based on the Fibonacci sequence. (a)–(c) $n=0$ and (d)–(f) $n=1$. Electric field, from left to right, is equal to 1.9, 2.2, and 2.5×10^{-6} a.u.

region of the phase space and it leads to overlapping of these functions as shown in Figs. 3(b) and 3(e). In this case we may express the electronic states by the linear superposition of individual states: $|\psi\rangle = a_0|\psi_0\rangle + a_1|\psi_1\rangle$, where $|a_0|^2 + |a_1|^2 = 1$. Using the definition given by Eq. (4) we obtain expression for the Wigner distribution function of the electronic state in the form

$$f(x,k) = |a_0|^2 f_0(x,k) + |a_1|^2 f_1(x,k)$$
$$+ 2\Re\left\{ a_0 a_1^* \int dx' \left\langle x - \frac{x'}{2} \middle| \psi_1 \right\rangle \left\langle \psi_0 \middle| x + \frac{x'}{2} \right\rangle e^{ikx'} \right\}. \quad (7)$$

The first two terms correspond to individual electronic states and the last term represents the mixture part which results from the bilinearity of the Wigner distribution function. This type of term is often termed the quantum interference.[59,60]

Quantitative analysis of the transition between electronic states $|\psi_n\rangle$ and $|\psi_m\rangle$ may be based on the product of their Wigner distribution functions $f_n(x,k)$ and $f_m(x,k)$ integrated over the phase space,[59–61] namely,

$$P_{nm} = 2\pi \int dx\, dk\, f_n(x,k) f_m(x,k). \quad (8)$$

The results of calculations of the overlapping integral given by Eq. (8) for the three lowest states in the Fibonacci chain are shown in Fig. 4. The maximum values of the overlapping integrals in both cases correspond to the electric field values at which the anticrossings between the appropriate states are observed. After a further increase in the electric field the quantum interference term disappears because the distance between states becomes larger and finally both states are well separated in the phase space which means that the overlapping integrals tend to zero. A similar situation is observed for the electronic states in the Thue-Morse chain, for example, in case of the Wigner functions shown in Fig. 5.
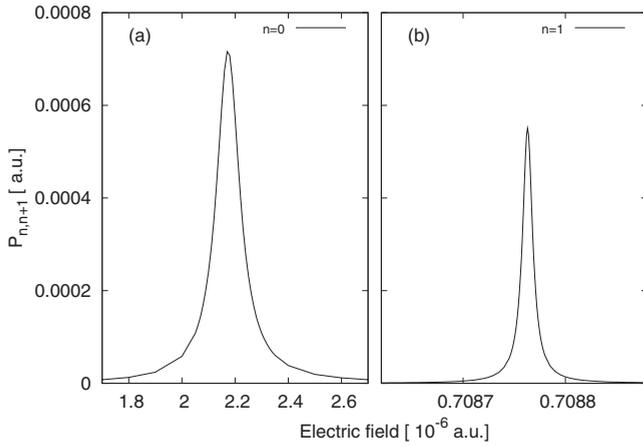
FIG. 4. The transition probability between the states n and $n+1$ at the bottom of the conduction band in the system based on the Fibonacci sequence; (a) $n=0$ and (b) $n=1$.

A more complex situation is presented in Fig. 6 where the evolution of the Wigner distribution functions for three quantum states in the vicinity of the middle of the conduction band is shown as a function of the electric field. In this case the energy spectrum (see Fig. 2) exhibits two anticrossings located close to each other. Each of these anticrossings mixes only two neighboring electronic states, therefore this process can be explained by the previous analysis. As it is presented in Figs. 3, 5, and 6 quantum states in the aperiodic chains under the fixed boundary conditions localize in limited areas of the phase space. The extents of these areas depend on the assumed distribution of the potential wells (based on Fibonacci or Thue-Morse sequence) and the number of quantum state.

One of the possibilities of measuring the degree of localization is to use the IPR parameter calculated in-phase space, defined by[46,47]
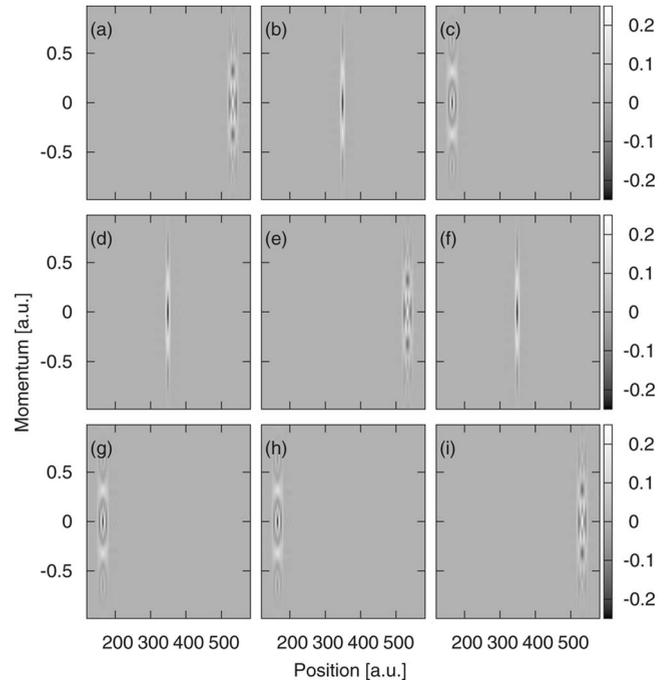

FIG. 5. The Wigner function for the system based on the Thue-Morse sequence. (a) and (b) E_F; (c) and (d) E_{F+1}. Electric field: (a) and (c) 0.98×10^{-6} a.u.; (b) and (d) 0.99×10^{-6} a.u.

FIG. 6. The Wigner function for the system based on the Fibonacci sequence. (a)–(c) E_{F-1}, (d)–(f) E_F, and (g)–(i) E_{F+1}. Electric field, from left to right, 1.8, 1.85, and 1.9×10^{-6} a.u.

$$\text{IPR}_n = \frac{1}{2\pi} \int dx dk [g_n(x,k;1/2)]^2, \qquad (9)$$

where $g_n(x,k;1/2)$ is the Husimi function. The Husimi function is an example of the non-negative nonclassical distribution functions, which can be obtained by the convolution of the Wigner distribution function and a window function[62]

$$g_n(x,k;\Delta_{xk}) = \int dx' dk' W(x-x',k-k';\Delta_{xk}) f_n(x',k'), \qquad (10)$$

where $W(x-x',k-k';\Delta_{xk})$ is a window function with resolution Δ_{xk}. In particular, the Husimi function is obtained if we choose the window function as a Gaussian function with the resolution corresponding to the minimum resulting from the uncertainty principle ($\Delta_{xk}=1/2$).

IPR can be used to study the influence of the electric field on localization, as shown in Fig. 7. For the ground state in the Fibonacci chain [see Fig. 7(b)] it was found that after IPR reaches the value of 0.13, further increase in the electric field to 2×10^{-6} a.u. does not change the localization. In a similar way, for the first excited-state IPR stabilizes initially at 0.08 for the fields larger than 0.7×10^{-6} a.u. Then, when the electric field is between 2 and 2.5×10^{-6} a.u., we observe that the energy levels values plotted versus the electric field change their gradient [see Fig. 2(b)]. This behavior is connected with the anticrossing taking place between the mentioned values of the electric field. In the phase space, the shape of the states changes, as well as the occupied area. Both states are shifted and the degree of localization changes significantly. As a consequence, the first excited state local-
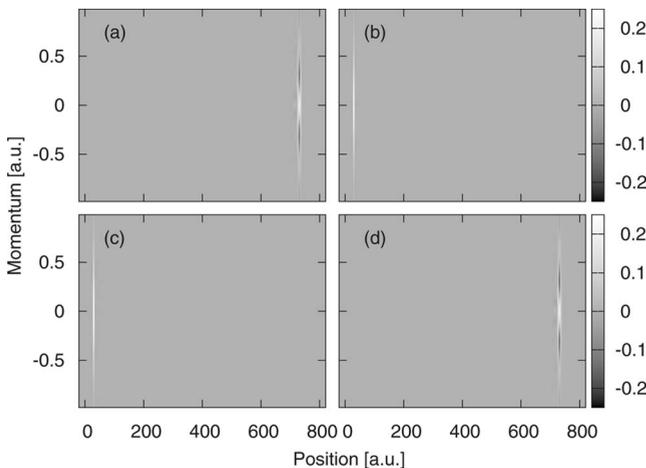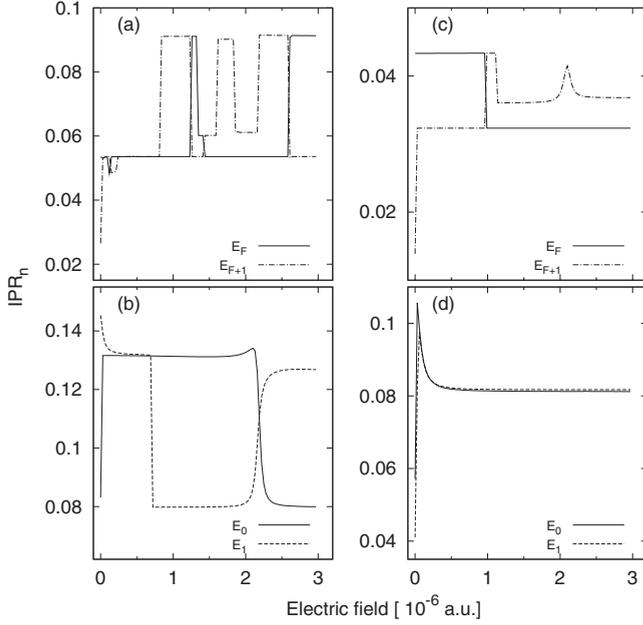
FIG. 7. Inverse participation ratio (IPR_n) for (a) and (b) the Fibonacci sequence and (c) and (d) Thue-Morse sequence.

izes in the region of the phase space previously occupied by the ground state and vice versa. The expectation values of the position and squared momentum presented in Figs. 8 and 9 were calculated for these states. The results confirm that the electric field shifts the states only at the points of anticrossings.

In case of the Thue-Morse sequence the observed behavior is slightly different. When the electric field is applied, localization of the two lowest states starts to increase very quickly and the states are shifted. Then, the degree of localization falls down and finally settles at a constant level. Also the expectation values of position and momentum do not undergo any further changes when the electric fields are increased. Similar characteristics of the ground state and the first excited state mean that increasing the electric field separates energies of the states, as shown in Fig. 2(d).

Figures 7(a) and 7(c) present changes in localization of the states from the middle of the band. The changes are very
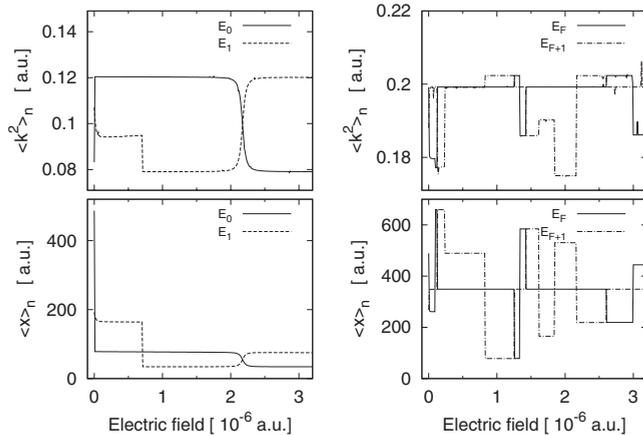

FIG. 8. The average position $\langle x \rangle_n$ and squared momentum $\langle k^2 \rangle_n$ for the Fibonacci sequence.
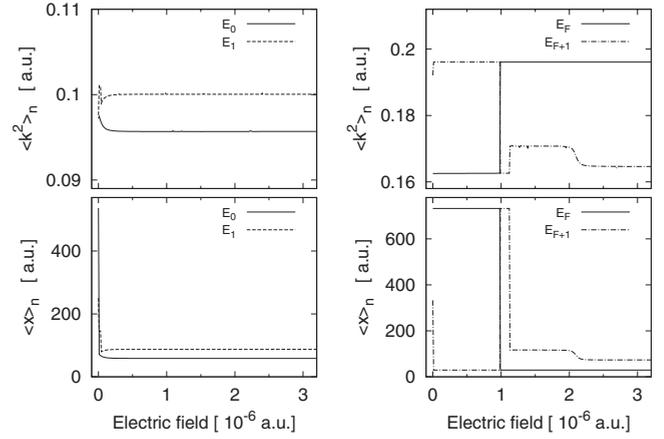

FIG. 9. The average position $\langle x \rangle_n$ and squared momentum $\langle k^2 \rangle_n$ for the Thue-Morse sequence.

sharp and are observed for the electric field values at which the plot of energy of the state against the electric field alters its gradient. Modification of the phase-space areas occupied by the states observed at the anticrossings, together with the change in IPR values, are caused by the decreasing of the energy between the states. For that reason we expect the quantum effects to have a greater impact on the analyzed states, notably the quantum interference between them. Appearance of that kind of effect should be accompanied by an increase in the negative part of the Wigner function, which is responsible for the quantum interference.

To investigate this phenomenon we split up the Wigner distribution function into two parts, namely,

$$f_n(x,k) = f_n^+(x,k) + f_n^-(x,k), \qquad (11)$$

where $f_n^+(x,k)$ and $f_n^-(x,k)$ correspond to the positive part and the negative part of the Wigner distribution function, respectively.

The measure of the nonclassical nature of an electronic state $|\psi_n\rangle$ is defined by the formula[57,58]

$$\nu_n = 1 - \frac{\mathcal{I}_n^+ - \mathcal{I}_n^-}{\mathcal{I}_n^+ + \mathcal{I}_n^-}, \qquad (12)$$

where $\mathcal{I}_n^+$ and $\mathcal{I}_n^-$ are the moduli of the integrals of the positive part and the negative part of the Wigner distribution function, respectively. Influence of the electric field on the ν_n parameter is shown in Fig. 10.

In the Fibonacci chain the nonclassical character considerably decreases (to about 0.52) immediately after turning the electric field on. Then its value does not change until the anticrossing takes place in the energy spectrum, where the ν_n parameter rises as a result of the increasing Wigner function negative part for both states. For a further increase in electric field the nonclassical nature decreases.

For the ground state in the Thue-Morse chain a monotonic decrease in the parameter ν_n is observed. It can be explained on the basis of large separation in the phase space between the ground state and the excited states.

States placed in the middle of the band also exhibit jumps of the nonclassical behavior at the electric fields at which the
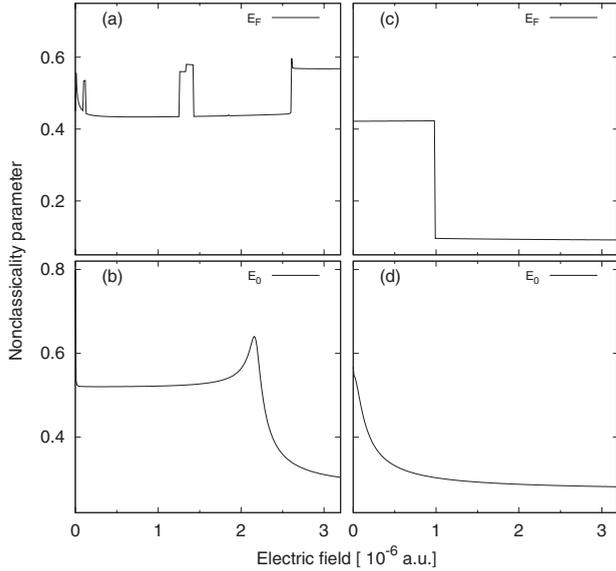
FIG. 10. The nonclassicality parameter ν_n calculated for the ground state $(n=0)$ in case of (b) the Fibonacci sequence and (d) Thue-Morse sequence. The nonclassicality parameter ν_n calculated for the states corresponding with the Fermi level in case of (a) the Fibonacci sequence and (c) Thue-Morse sequence.

anticrossings are observed. Here, however, the widths of anticrossings are very small and the numerical accuracy does not allow to illustrate the peaks of nonclassicality parameter but only to show the values below and above anticrossings.

Additionally we calculate the standard deviations of position and momentum variables that are defined by expressions: $\sigma_n^2(x)=\langle x^2\rangle_n-\langle x\rangle_n^2$ and $\sigma_n^2(k)=\langle k^2\rangle_n-\langle k\rangle_n^2$, respectively, applying Eq. (5) to find the relevant quantities from the Wigner function $f_n(x,k)$. The acquaintance of these deviations allows one to calculate the uncertainty product $\sigma_n(x)\sigma_n(k)$ as a function of the electric field. Figure 11 shows results for the uncertainty product for the two lowest states in both aperiodic chains. We may see that the electric field produces rapid changes in the uncertainty product around the anticrossings for both states. This behavior of the uncertainty product can be explained by the highly nonclassical features
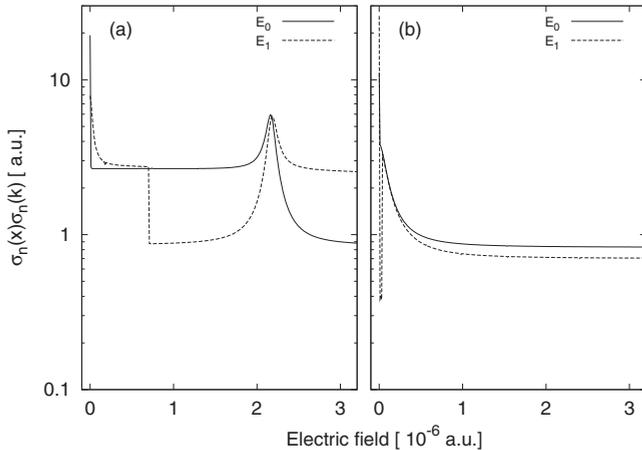

FIG. 11. The product of the position and momentum variances for the (a) Fibonacci sequence and (b) the Thue-Morse sequence.

of the Wigner distribution function corresponding to the quantum state in the region of anticrossing where the quantum interference phenomena play important role. On the other hand the uncertainty product allows one to distinguish between pseudoclassical and nonclassical states. It results from the fact that the uncertainty product is equal to 1/2 for the coherent states, which are recognized as the states closest to classical ones. Hence the nonclassical states may be characterized by the uncertainty product greater than 1/2. As it presented in Fig. 11, the uncertainty product is usually greater than one which means that the discussed states are nonclassical.

IV. CONCLUDING REMARKS

We have studied the influence of the homogeneous electric field on the energy spectrum of the finite one-dimensional aperiodic systems generated by the Fibonacci and Thue-Morse sequences. We have shown that the homogeneous electric field modifies the energy spectrum of aperiodic systems and leads to the formation of the subbands. The appearance of subbands is a consequence of the attraction between energy levels for some value of the electric field. The anticrossings are observed for these values of the electric field.

We have applied the phase-space method based on the Wigner distribution function to analyze the region of anticrossings for the lowest electronic states in both aperiodic systems. The discussion of the electronic states in the middle of conduction band is also included. This formulation allows us to investigate the nonclassical properties of the electronic states and their influence on the transitions between them. We have shown that the nonclassical properties of electronic states of the aperiodic systems under the homogeneous electric field are most profound in the regions of anticrossings. The increase in the nonclassical parameter in these regions is a consequence of the increasing role of the negative part of the Wigner distribution function and it is correlated with the changes in the localization properties of electronic states and the dynamical variables. Finally, we have used the uncertainty product of momentum and position variables as a simple measure of nonclassicality of the electronic state. We have found that this product as a function of the electric field is also correlated with the nonclassical properties of electronic states in the aperiodic systems. In the paper we have paid attention to the aperiodic systems in the limit of low homogeneous electric field. The limit of strong electric field and dynamical aspect of the problem will be included in forthcoming publications.

*spisak@novell.ftj.agh.edu.pl

†woloszyn@agh.edu.pl

[1] D. M. Eigler and E. K. Schweizer, Nature (London) **344**, 524 (1990).

[2] G. Meyer Jascha Repp, Sven Zöphel, Kai-Felix Braun, Saw Wai Hla, Stefan Fölsch, Ludwig Bartels, Francesca Moresco, and Karl Heinz Rieder, Single Mol. **1**, 79 (2000).

[3] C. J. Muller, J. M. van Ruitenbeek, and L. J. de Jongh, Physica C **191**, 485 (1992).

[4] A. I. Yanson, G. Rubio-Bollinger, H. E. van den Brom, N. Agrait, and J. M. van Ruitenbeek, Nature (London) **395**, 783 (1998).

[5] R. H. M. Smit, C. Untiedt, A. I. Yanson, and J. M. van Ruitenbeek, Phys. Rev. Lett. **87**, 266102 (2001).

[6] H. Ohnishi, V. Kondo, and K. Takayanagi, Nature (London) **395**, 780 (1998).

[7] J. Bettini, F. Sato, P. Z. Coura, S. O. Dantas, D. S. Galvao, and D. Ugarte, Nat. Nanotechnol. **1**, 182 (2006).

[8] J. N. Crain, J. L. McChesney, F. Zheng, M. C. Gallagher, P. C. Snijders, M. Bissen, C. Gundelach, S. C. Erwin, and F. J. Himpsel, Phys. Rev. B **69**, 125401 (2004).

[9] M. Krawiec, T. Kwapiński, and M. Jałochowski, Phys. Rev. B **73**, 075415 (2006).

[10] B. L. Altshuler, A. G. Aronov, D. E. Khmelnitskii, and A. I. Larkin, in *Quantum Theory of Solids*, edited by I. M. Lifshits (MIR, Moscow, 1982).

[11] P. A. Lee and T. V. Ramakrishnan, Rev. Mod. Phys. **57**, 287 (1985).

[12] B. Kramer and A. MacKinnon, Rep. Prog. Phys. **56**, 1469 (1993).

[13] G. H. Wannier, Phys. Rev. **117**, 432 (1960).

[14] J. E. Avron, Ann. Phys. **143**, 33 (1982).

[15] G. Nenciu, Rev. Mod. Phys. **63**, 91 (1991).

[16] V. Grecchi and A. Sacchetti, Ann. Phys. **241**, 258 (1995).

[17] E. E. Mendez, F. Agulló-Rueda, and J. M. Hong, Phys. Rev. Lett. **60**, 2426 (1988).

[18] P. Voisin, J. Bleuse, C. Bouche, S. Gaillard, C. Alibert, and A. Regreny, Phys. Rev. Lett. **61**, 1639 (1988).

[19] M. Ghulinyan, C. J. Oton, Z. Gaburro, L. Pavesi, C. Toninelli, and D. S. Wiersma, Phys. Rev. Lett. **94**, 127401 (2005).

[20] W. Shockley, Phys. Rev. Lett. **28**, 349 (1972).

[21] H. Fukuyama, Phys. Rev. B **8**, 5579 (1973).

[22] C. L. Roy and P. K. Mahapatra, Phys. Rev. B **25**, 1046 (1982).

[23] C. M. Soukoulis, J. V. Jose, E. N. Economou, and P. Sheng, Phys. Rev. Lett. **50**, 764 (1983).

[24] V. N. Prigodin and B. L. Altshuler, Phys. Lett. A **137**, 301 (1989).

[25] C. S. Ryu, G. Y. Oh, and M. H. Lee, Phys. Rev. B **48**, 132 (1993).

[26] P. E. de Brito, C. A. A. da Silva, and H. N. Nazareno, Phys. Rev. B **51**, 6096 (1995).

[27] R. Farchioni and G. Grosso, Phys. Rev. B **56**, 1981 (1997).

[28] M. Glück, A. R. Kolovsky, H. J. Korsh, and N. Moiseyev, Eur. Phys. J. D **4**, 239 (1998).

[29] B. Rosam, D. Meinhold, F. Löser, V. G. Lyssenko, S. Glutsch, F. Bechstedt, F. Ross, K. Köhler, and K. Leo, Phys. Rev. Lett. **86**, 1307 (2001).

[30] M. Glück, A. R. Kolovsky, and H. J. Korsh, Phys. Rep. **366**, 103 (2002).

[31] M. Kast, C. Pacher, G. Strasser, E. Gornik, and W. S. M. Werner, Phys. Rev. Lett. **89**, 136803 (2002).

[32] A. Zhang, L. C. Lew Yan Voon, and M. Willatzen, Phys. Rev. B **73**, 045316 (2006).

[33] V. I. Tatarskii, Sov. Phys. Usp. **26**, 311 (1983).

[34] M. Hillery, R. F. O'Connell, M. O. Scully, and E. P. Wigner, Phys. Rep. **106**, 121 (1984).

[35] H.-W. Lee, Phys. Rep. **259**, 147 (1995).

[36] W. P. Schleich, *Quantum Optics in Phase Space* (Wiley VCH, Weinheim, 2001).

[37] J. M. Luck, Phys. Rev. B **39**, 5834 (1989).

[38] A. Bovier and J.-M. Ghez, Commun. Math. Phys. **158**, 45 (1993).

[39] B. Hu, B. Li, and P. Tong, Phys. Rev. B **61**, 9414 (2000).

[40] G. J. Morgan, M. Howson, and K. Saub, J. Phys. F: Met. Phys. **15**, 2157 (1985).

[41] W. R. Frensley, Rev. Mod. Phys. **62**, 745 (1990).

[42] B. A. Biegel and J. D. Plummer, Phys. Rev. B **54**, 8070 (1996).

[43] C. Jacoboni and P. Bordone, Rep. Prog. Phys. **67**, 1033 (2004).

[44] P. Wójcik, B. J. Spisak, M. Wołoszyn, and J. Adamowski, Acta Phys. Pol. A **114**, 1431 (2008).

[45] B. J. Spisak and M. Wołoszyn, Acta Phys. Pol. B **38**, 1951 (2007).

[46] G.-L. Ingold, A. Wobst, Ch. Aulbach, and P. Hänggi, Lect. Notes Phys. **630**, 85 (2003).

[47] M. Wołoszyn and B. J. Spisak, Mater. Sci. (Poland) **22**, 545 (2004).

[48] S. R. Wilkinson, C. F. Bharucha, K. W. Madison, Q. Niu, and M. G. Raizen, Phys. Rev. Lett. **76**, 4512 (1996).

[49] K. W. Madison, M. C. Fischer, and M. G. Raizen, Phys. Rev. A **60**, R1767 (1999).

[50] J. Billy, V. Josse, Z. Zuo, A. Bernard, B. Hambrecht, P. Lugan, D. Clement, L. Sanchez-Palencia, Ph. Bouyer, and A. Aspect, Nature (London) **453**, 891 (2008).

[51] R. Perez-Alvarez, F. Garcia-Moliner, and V. R. Velasco, J. Phys.: Condens. Matter **13**, 3689 (2001).

[52] M. Glück, A. R. Kolovsky, H. J. Korsch, and F. Zimmer, Phys. Rev. B **65**, 115302 (2002).

[53] E. Macia, Rep. Prog. Phys. **69**, 397 (2006).

[54] G. H. Wannier, Rev. Mod. Phys. **34**, 645 (1962).

[55] A. S. Davydov, *Quantum Mechanics*, 1st ed. (Pergamon, Oxford, 1965).

[56] W. H. Zurek, Phys. Today **44** (10), 36 (1991).

[57] M. G. Benedict and A. Czirják, Phys. Rev. A **60**, 4034 (1999).

[58] A. Kenfack and K. Życzkowski, J. Opt. B: Quantum Semiclassical Opt. **6**, 396 (2004).

[59] J. P. Dowling, W. P. Schleich, and J. A. Wheeler, Ann. Phys. **503**, 423 (1991).

[60] G. S. Agarwal, Found. Phys. **25**, 219 (1995).

[61] D. Dragoman, Phys. Scr. **72**, 290 (2005).

[62] Q. S. Li, G. M. Wei, and L. Q. Lu, Phys. Rev. A **70**, 022105 (2004).